Journal of Visualization, Vol. 12, No. 4 (2009) 393-400

Regular Paper

Visualization of Flapping Wing of the Drone Beetle

Kitagawa, K.*[1], Sakakibara, M.*[2] and Yasuhara, M.*[1]

*1 Department of Mechanical Engineering, Aichi Institute of Technology, 1247 Yachigusa, Yakusa, Toyota, Aichi 4700392, Japan.
E-mail: kitagawa@aitech.ac.jp
*2 Graduate student, Department of Mechanical Engineering, Aichi Institute of Technology, Japan.

Received 14 October 2008
Revised 4 April 2009

Abstract : Investigation of flapping wings of insect are focused on low Reynolds number effect and the unsteady aerodynamic properties. Interaction between flapping wing of insects and the air flow became one of important and fundamental research topics in micro air vehicle. The present work is aim to investigate the flow behavior of flapping wings of tethered scarab beetle. The generation mechanisms of velocity field and vortex formation are visualized with smoke-wire method. Tethered flight of the drone beetle shows the motion with elastic deformation of flapping wing. Measured flapping frequency is about 71 Hz and its frequency is higher than for dragonfly and butterfly. Beetle decreases negative lift by feathering motion in the upstroke process and increase positive lift by effect of wake capture in the downstroke process.

Keywords : insect flight, drone beetle, flow visualization, biofluid mechanics, micro air vehicle

1. Introduction

Aerodynamic properties of insect's flight and hydrodynamic properties of swimming fish draw the attention of many researchers. The researchers have been investigating unmanned aerial vehicles (UAV), micro air vehicles (MAV) and biologically inspired flight systems (BIFS). MAVs could be used in an earthquake and fire environment, biological, chemical and radioactive contamination to conduct reconnaissance in areas inaccessible to human or other methods. Many civilian, commercial and scientific applications exist for MAVs, including traffic monitoring, accident assessment, exploratory research, wildlife, land management and scientific space exploration. In order to develop insect-like flapping-wing MAVs must collect for data of flying motion and flow around wing and body. The complex three dimensional dynamic structures of leading edge vortex (LEV) and spanwise flow generated by flapping wings in insect flights is incompletely understood. The insect wing have deformable structure, which resulted in essential changes in wing shape as a function of angle of attack and unsteady aerodynamic forces. The flow-adaptable wing is thought to provide enhanced vehicle stability and wind gust alleviation compared to rigid wing. Aerodynamic mechanisms of living insects or birds flight were investigated experimentally and numerically by many researchers. Insects offer biologists a range of useful examples to elucidate evolutionary constraints in organismal (Brodsky, 1994). Ellington (1984) investigated the mean lift coefficient required during hovering flight from rotary wing aerodynamics. Azuma and Watanabe (1988) showed that dragonfly flight explained by steady-state aerodynamics. Dickinson (1996) carried out flow visualization and in-

stantaneous force measurements of tethered fruit flies to study the dynamics of force generation during the flight. Willmott et al. (1997) investigated smoke visualization study of tethered hawkmoth. The wing motion model of fruit fly was investigated by computational fluid dynamics approach (Sun and Tang, 2002). The mechanism of lift enhancement of hawkmoth was confirmed by computational fluid-dynamic analyses (Liu et al., 1998). Study of aerodynamic property in flying beetle were generally lacking in sufficient precision in visualizing flow filed. Souza et al. (1997) are discussed aerodynamic stabilization by beetle elytra. Burton (1964) investigated turning mechanisms of rhinoceros beetles. Beetles have one pair of forewings and membranous hindwings. The flight styles of most beetles extend elytra, and unfold and flap soft hindwing laterally during flight. The elytra are held at a pronounced dihedral angle. Interaction between these wings and air flow makes complex three dimensional flow structure. Distinction of beetle has a large volume comparison of dragonfly and butterfly. For development of MAV, its body appears useful space for electrical and flapping equipment of power and exploration systems. An aerodynamic property of species of beetle was not strictly discussed for flapping motion and flow behavior. The motivation of present study is to investigate flying mechanism of live drone beetle, such as *Anomala cuprea*. The first report of this study presents experimentally investigation for tethered flight of live drone beetle by wing motion and air flow visualization. Tethered flight experiments for live insect were conducted using high speed video recording and smoke-wire method.

2. Drone beetle and Experimental Apparatus

2.1 Drone beetle

Figure 1 show photographs of the drone beetle. The drone beetle, such as scarab beetle species *Anomala cuprea* is commonly known as the Japanese beetle. *Anomala cuprea* was collected near a grove in Gifu prefecture, Japan. It has one pair of hard forewings (elytron) and membranous hindwings, pronotum and scutellum as shown in Figs. 1 and 2. In Fig. 1, the front pair of wings in beetles is sclerotised (hardened) to form elytron and they protect the delicate soft hindwings which are folded beneath. *Anomala cuprea* has 22.8±1.37 mm in body length, 12.1±0.72 mm in width, 0.89 ±0.16 g in net mass by the standard deviation, about 13.5 mm in wing length and 6 mm in wing span(chord) for forewing, 21 mm in wing length, 8 mm in wing span(chord) and 6.0 in aspect ratio (=wing span^2/wing area) for hindwing, respectively.

Micrograph of the surface of the insect wing and body were conducted using a CCD microscope (KEYENCE CO., VW-6000). The surface roughness of insect was observed and photographed by CCD camera. Figure 2 show the scanning CCD image of micrograph of drone beetle. The forewing has rigid surface with many small dimple on elytrons, pronotum and scutellum. The hindwing has a number of longitudinal veins, bristle and nodus of leading edge and many creases of trailing edge. Its neck, nodus and leg have a lot of bristles. The size of dimple on pronotum are about 0.06 mm in diameter of dimple, and 0.12 mm in pitch of dimple, respectively.

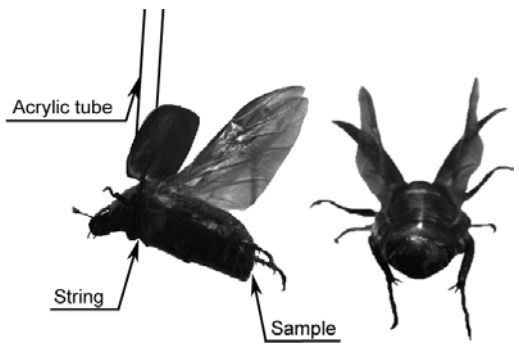

Fig.1. Photographs of *Anomala cuprea*.

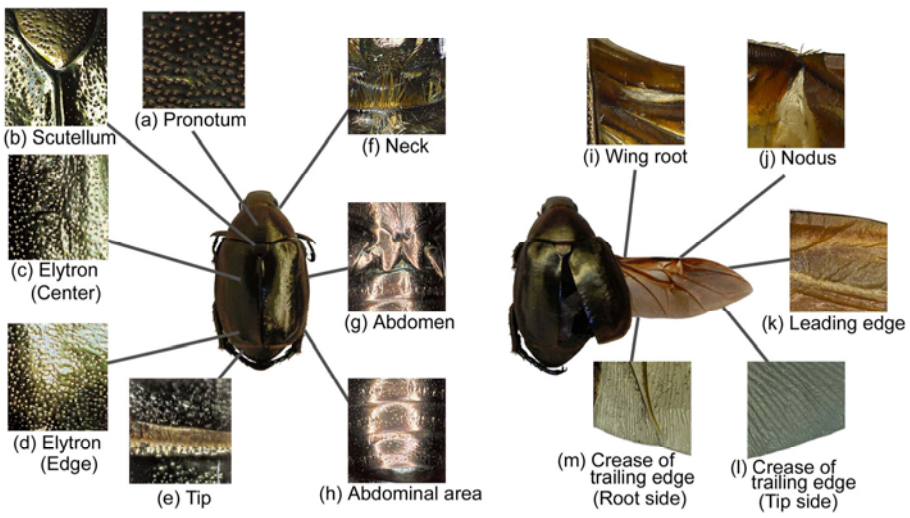

Fig.2. Surface shape of drone beetle.

2.2 Low speed Wind tunnel

Tethered flight experiments on the visualization of flow field around the flapping wing are conducted in Eiffel type low speed wind tunnel, as shown in Fig. 3. The low speed wind tunnel has a square cross section of 150 × 150 mm and 2600 mm in length, respectively. Figure 4 shows experimental setup of the test section. It consists of a 150 × 150 mm acrylic channel enclosed by 5 mm of thick wall. The 600 mm thickness of open cell type polyurethane foam layer was inserted in the upstream of the test section. Polyurethane foam is of products of Bridgestone Co., Japan. The cells are connected through each open faces, and passage of gas is possible from one cell to the next. Each cell of the foam is composed of irregularly lopped thin wire, connected three-dimensionally, as shown in Fig. 5.

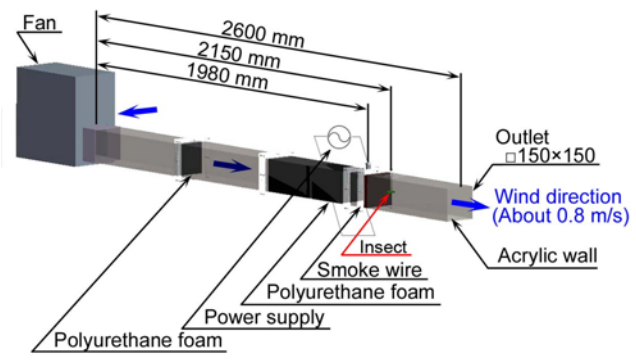

Fig.3. Experimental setup of Eiffel type low speed wind tunnel in AIT.

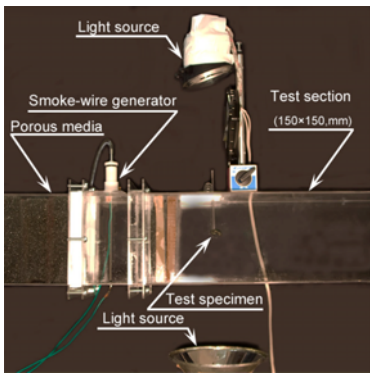

Fig.4. Photograph of test section.

2.3 Flow visualization of tethered flight

An acrylic window provides a view field of 150 × 600 mm when a drone beetle inserted and tethered in the test section. During the experiment on the measurement of flapping motion and streamlines, a live insect with string attached to its body mounted in the test section of wind tunnel, as shown in Fig. 1. The insect is suspended by string covered with hollow acrylic tube. The outer and inner diameters of an acrylic tube are 3.0 mm and 2.0 mm, respectively. The smoke-wire technique is an ideal method to visualize the three-dimensional flow field. When the wire was electrically heated, it vaporizes the silicon oil and releases the vapor into the flow. The oil produces smoke filaments when it condenses into visible whitish cloud of hot oil vapor. The high speed video camera (High Speed Star-6 : HSS-6, LaVision) with the resolution of 768 × 768 pixels was used for all video recording. Lens

was used 55 mm macro lens (Nikon) at F = 3.5. The flow field is illuminated using high intensity discharge lamps positioned at the top and bottom sides of view section, before view window the top sides of the insect, as shown in Fig. 4. Footage of the smoke was captured by one of the high speed video camera operating at various shutter speeds, and the individual images were transferred to a computer. Figure 6 shows focal plane of smoke wire method. Each photograph is used to visualize airflow motion on central part of wing span.

Fig.5. Micrograph of polyurethane foam.

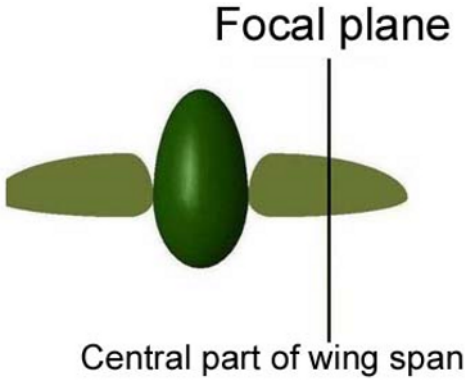

Fig.6. Focal plane on wing center for flow visualization.

3. Results and Discussion

3.1 Wing motion of a tethered flight in scarab beetle

The wing flap creates swirls of air flow and generates aerodynamic forces that allow insects to dart forward, to turn, and to hover. The tethered flight differences typical feeding flight, such as flapping frequency and flow behavior. Figure 7 show one complete wing stroke images during a steady tethered flight of *Anomala cuprea*. Each photograph is an interframe time of $\Delta t = 0.50$ msec. The camera was operated at a speed of 10,000 fps. It is seen from these photographs that, the tethered drone beetle clearly show the wing motion (downstroke/upstroke) and elastic deformation of hindwing in the view field. One complete cycle of flapping lasts about 10 msec, which can be divided into several phases of wing motions: feathering, clap-and-fling, upstroke process in frames 1-15 and downstroke process in frames 16-28. In Fig.7, bottom dead center (B.D.C) in frame 2 and the top dead center (T.D.C) and clap-and-fling motion observed in frames 14-16. At the beginning of the flight, the hindwings are rising to horizontal plane at high angle of attack. Feathering motion occurs in frames 5-6 and the wing changes the local angle of attack. The flapping motion with feathering generate large lifting force, it is enough to lift the insect. The wing alters the large local angle of attack, breaks up the airflow close to the leading edge, and regulates the air flow off the wing. Durations of the clap-and-fling occurs in frames 14-16. Weis-Fogh (1973) proposed to generate instantaneously a large wing lift by clap-and-fling motion. A detailed theoretical analysis of the clap-and-fling can be found in Lighthill (1973). Then the drone beetle rise lift by flapping motion with feathering and the Weis-Fogh mechanism. Chord Reynolds number (R_{ec}) is based on insect wing chord length and flight velocity is usually used to characterize the aerodynamic performance of an airfoil/wing. In the present study, the velocity of the incoming flow was set as $U_\infty = 0.8$ m/s, which corresponds to a chord Reynolds number of $R_{ec} = 389$. Local Reynolds number (R_{eL}) is defined as wing chord length and maximum flapping velocity. The maximum flapping velocity measured from high speed image as $U_\infty = 4.6$ m/s and wing chord is of 8 mm, which corresponds to a local Reynolds number of $R_{eL} = 2.23\times10^3$. In insect flight, the flapping velocity is faster than its flight speed. Therefore the aerodynamic force depends on the flapping velocity. Figure 8 show experimental results of hindwing tip motion and angle of attack of tethered flight of *Anomala cuprea*. The solid lines denote flapping motion during one period stoke, the red lines the upstroke, blue lines the downstroke and small circles mark the leading edge.

The angle of attack is changing during the flapping motion, lift and drag forces are instantaneously changed. Wing motion indicates the instantaneous position at 28 temporally equidistant points during one period stroke.

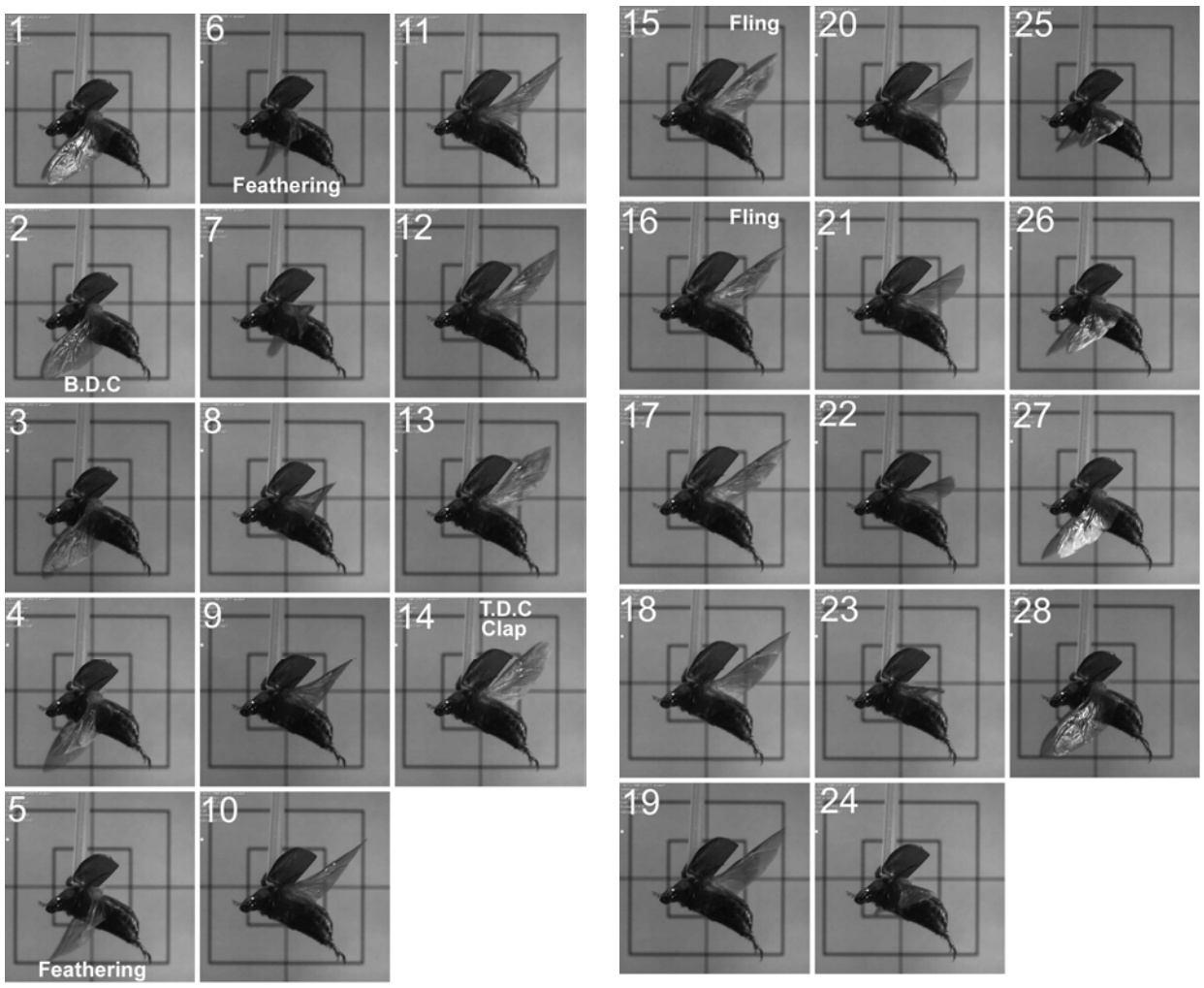

Fig.7. Slow motion pictures of a tethered *Anomala cuprea* during one period stroke with an interframe time of Δt = 0.50 msec.

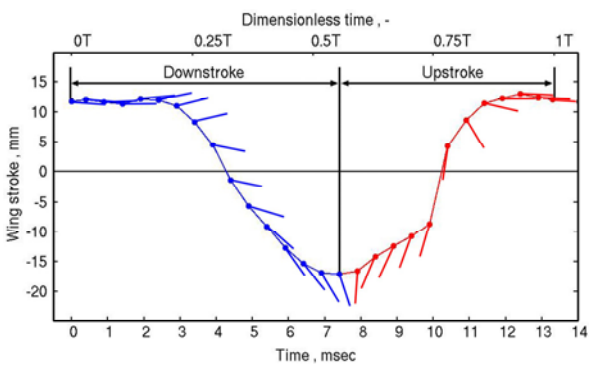

Fig.8. Wing stroke – time diagram of hindwing tip motion and angle of attack.

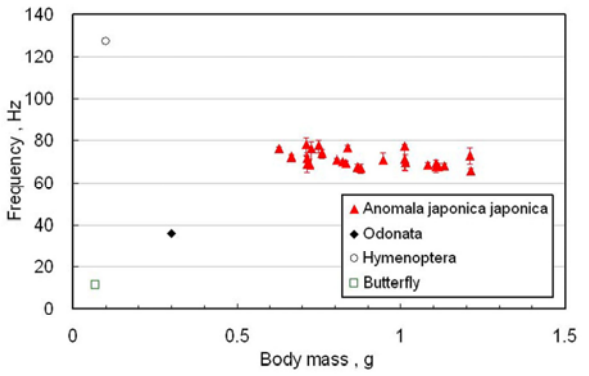

Fig.9. Relation between body mass and flapping frequency.

The wing stroke is a cosine like curve whose T.D.C, B.D.C and wing stroke are 13 mm, -19 mm and 32 mm, respectively. The angles of attack α = 107 degrees at mid upstroke, α = 17 degrees at mid downstroke, α = 3 ~ 5 degrees at T.D.C and α = 72 degrees at B.D.C were maintained throughout. In

the flight of drone beetle, the feathering angle was differenced at upstroke and downstroke process, which controlled the generation of the LEV. Figure 9 show relations between body mass and flapping frequency for several insects. The red triangles denote the *Anomala cuprea*, the lozenge the *Odonata* in the dragonfly, the circle the *Hymenoptera* in the bee and square the butterfly. Body mass of *Anomala cuprea* is the largest of the other insects. Measured flapping frequency is measured about 71 ± 12 Hz by the standard deviation 3. It is apparent from Fig. 9 that, in between m = 0.6 ~ 1.2 g, the flapping frequency are nearly constant value of 71 Hz with the increase in body mass.

3.2 Flow Visualization of a tethered flight

Figure 10 show visualizations of streamline around the central part of wing span for a tethered flight of *Anomala cuprea*. Each photograph is visualized airflow motion on central part of wing span and an interframe time of Δt = 0.50 msec. The camera was operated at a speed of 10,000 fps. Streamlines around a flapping wing and insect body were visualized by smoke-wire method with high speed video recording. The wind direction indicate right hand. Flow velocity is about 0.8 m/s at test section in wind tunnel. The upstroke process denotes in frames 1-15 and the downstroke process in frames 16-28. The smoke streams have thinned and become closer, indicating that the air flow has higher velocity than inlet velocity. Figure 11 show schematic representations of wake features during downstroke (B.D.C) and upstroke (T.D.C). Solid arrows show the air flow, including the circulation around vortex tubes and the dotted lines region of vortex. When the downstroke and upstroke reverse, upstroke starting vortex (USV) is created with clockwise circulation at frame 4. After at frame 5, USV grow up more intense circulation as the half stroke process. In Fig. 10, airflow on its body is accelerated through downstroke tip vortex (DTV) by the clap-and-fling. The clap-and-fling of hindwing are cutting through the smoke lines nearly T.D.C, generating tip vortex. The tip vortex left in the wake where the tip has passed through the smoke streams provides confirmation that bound circulation is produced during the upstroke. The trailing edge region of hindwing remains impervious to fluid throughout the motion of the fling. The mechanism of insect flight, twisting motion (feathering) of flapping wing conducted an important role in generating aerodynamic lift. The feathering motions control angle of attacks of the flapping wing and reduced negative lift in the upstroke process (Dickinson et al., 1999). In the upstroke process, the drone beetle decreases negative lift by feathering motion, while in the downstroke process, they rise positive lift by the effect of wake capture. DTV and USV moved downstream towards off the end of the body. At the mid downstroke process, LEV is generated and accelerated through downstream. The wake structure of DTV and USV are interacting and colliding to break down vortex while the leading edge vortex is grew strong swirl flow. During the end of downstroke, DTV is created clockwise circulation over the upper surface of wing by feathering motion. The hard forewing is created auxiliary lift, while the membranous hindwing adjusts to the angle of attack and the pitching angle under the any flow condition and changes in aerodynamic force.

4. Conclusion

The flying mechanism of drone beetle is investigated experimentally to visualize wing motion and flow pattern during the unsteady process. Tethered flights of the drone beetle understand the motion of the wing (downstroke/upstroke) and elastic deformation of hindwing.

Anomala cuprea has many small dimples on elytrons, pronotum and scutellum. The hindwing folded beneath in hard forewing and deformed flexible membrane and longitudinal vein of wing structure. The hindwing has a number of longitudinal veins, bristle and nodus of leading edge and many creases of trailing edge. The most beetles extend elytra, and unfold and flap soft hindwings during flight. The flapping frequency of *Anomala cuprea* is about 71 ± 12 Hz and its frequency is higher than dragonfly and butterfly. Chord Reynolds number (R_{ec}) and local Reynolds number (R_{eL}) have 389

and 2.23×10^3, respectively. Experimental results show that *Anomala cuprea* has four phases of wing motions, feathering, clap-and-fling, upstroke and downstroke processes. The flying beetle uses circulation of tip vortex and obtains lift by feathering motion, while the membrane wing of beetle adjusts to the angle of attack and the pitching angle under changes in aerodynamic force. The hard forewing is created auxiliary lift. DTV and USV are created clockwise circulation over the upper surface of wing by feathering motion. The drone beetle decreases negative lift by feathering motion in the upstroke process and increase positive lift by the effect of wake capture in the downstroke process.

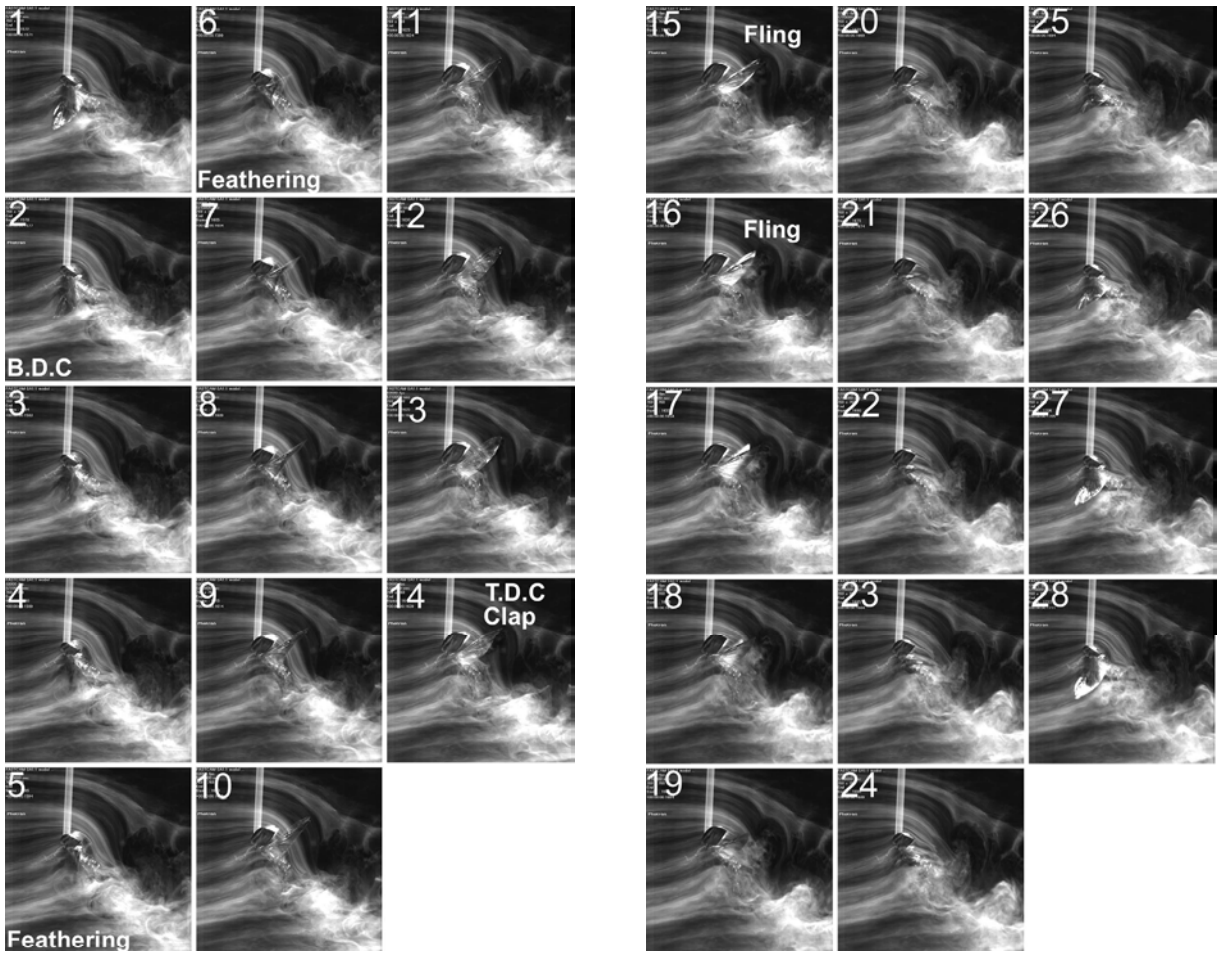

Fig.10. Smoke-wire visualization of steady flapping motion of a tethered *Anomala cuprea*.

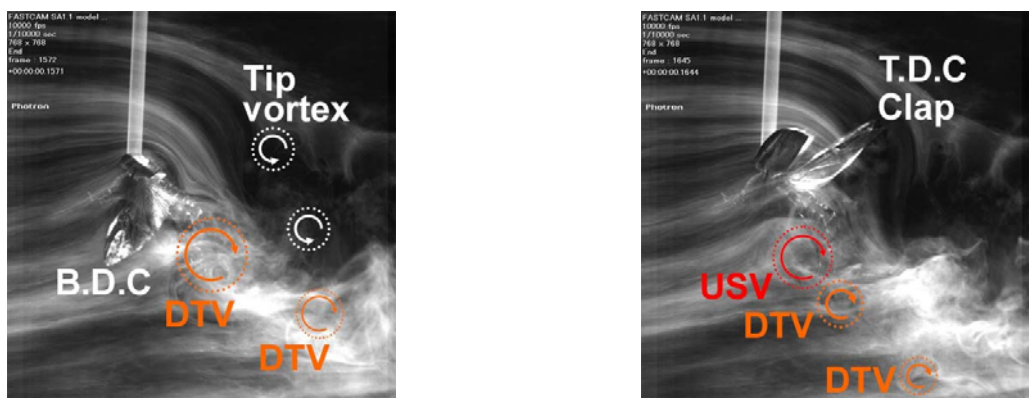

(a) B.D.C (b) T.D.C

Fig.11. A generalized model for wake structure. Schematic representations of the visualized wake features during B.D.C and T.D.C, respectively.

Acknowledgments

We would like to acknowledge the anonymous referees for their valuable comments and suggestions on the manuscript. High speed camera HSS-6 was provided by the KANOMAX Japan INC.

References

Azuma, A. and Watanabe,T., Flight Performance of a Dragonfly. J. Exp. Biol., 137 (1988), pp 221-225.
Burton, A. J., Nervous control of flight orientation in a beetle. Nature, Land(1964), 204, 1333.
Brodsky, A. K., The Evolution of Insect Flight. Oxford University Press, 1st edition, 1994.
Dickinson, M. H., The wake dynamics and flight forces of the fruit fly Drosophila melanogaster. J. Exp. Biol. 199(1996), pp 2085-2104.
Dickinson, M. H., Lehmann, F. O. and Sane, S. P., Wing rotation and the aerodynamic basis of insect flight. Science, 284 (1999), pp 1954-1960.
Ellington, C. P., The aerodynamics of hovering insect flight. III. Kinematics. Phil. Trans. R. Soc. Lond., 1984, pp 41-78.
Ellington, C. P., Berg, C. V. D., Willmott A. P. and Thomas, A. L. R., Leading-edge vortices in insect flight. Nature, 384 (1996), pp 626-630.
Lighthill, S. J., Mathematical Biofluiddynamics. University of Cambridge, 1975.
Liu, H. and Kawachi, K., A numerical study of insect flight, J. Comp. Phys., 146 (1998), pp 124-156,.
Liu, H., Ellington, C. P., Kawachi, K., Berg, V. D, and Willmott, A. P., A Computational Fluid Dynamics Study of Hawkmoth Hovering. J. Exp. Biol., 201 (1998), pp461-477.
Nakamura,M., Iida, A. and Mizuno, A., Visualization of Three-Dimensional Vortex Structures around a Dragonfly with Dynamic PIV, Journal of Visualization, 10-2 (2007), pp. 159-160.
Sudo, S., Tsuyuki, K., Ikohagi, T., Ohta, F., Shida, S. and Tani, J., A Study on the Wing Structure and Flapping Behavior of a Dragonfly. JSME Int. J., 42 (1999), pp 721-729.
Sun, M. and Tang, J., Unsteady aerodynamic force generation by a model fruit fly wing in flapping motion, J. Exp. Biol., 205 (2002), pp 55-70.
Sunada, S., Wachi, K., Watanabe, I. and Azuma, A., Performance of a butterfly in take-off flight. J. Exp. Biol., 183 (1993), pp 249-277.
Souza, M. M. and David. E. A., Unsteady aerodynamic force generation by a model fruit fly wing in flapping motion, J. Exp. Biol., 205 (2002), pp 55-70.
Walker, J. A., Rotational lift: something different or more of the same?, J. Exp. Biol., 205 (2002), pp 3783-3792.
Willmott, A. P., Ellington, C. P. and Thomas, A. L. R, Flow visualization and unsteady aerodynamics in the flight of the hawkmoth, Manduca sexta. Phil. Trans. R. Soc. Lond. B, 352 (1997), pp 303-316.
Weis-Fogh, T., Quick estimates of flight fitness in hovering animals, including novel mechanisms for lift production. J. exp. Biol. 59 (1973), pp 169-230.

Author Profile

Kazutaka Kitagawa: He received his Ph.D. in Mechanical Engineering in 1995 from Aichi Institute of Technology. He worked in Department of Mechanical Engineering, Aichi Institute of Technology as an assistant professor since 1996-2004, University of Kentucky as a visiting scholar in 2005 – 06 and Department of Mechanical Engineering, Aichi Institute of Technology as an associate professor since 2005. His research interests are supersonic flow, hypersonic flow, computational fluid dynamics, aerodynamics and biofluid mechanics.

Mitsutoshi Sakakibara: He is graduate student at Department of Mechanical Engineering, Aichi Institute of Technology. He received his Bachelor's degreesree in Department of Mechanical Engineering in 2007 from Aichi Institute of Technology. His research interests are aerodynamics and biofluid mechanics.

Michiru Yasuhara: He received his Bachelor's degreesree in 1951 from University of Tokyo and his Dr.(Eng) in 1962 from the same university. He worked in Department of Aerospace Engineering, Nagoya University as professor since 1967-91 and Cornell University as a visiting associate professor in 1963 - 65. He works in Department of Mechanical Engineering, Aichi Institute of Technology as professor since 1992. His research interests are hypersonic flow, rarefied gas dynamics, computational fluid dynamics and shock waves.